

3-D APPLIED ELEMENT METHOD FOR PP-BAND RETROFITTED MASONRY

**K. Worakanchana¹, P. Mayorca², R. Guragain³,
S. Navaratnanaj⁴ and K. Meguro⁵**

^{1,2} *Project researcher, International Center for Urban Safety Engineering, Institute of Industrial Science, the University of Tokyo, Japan*

³ *Director, Earthquake Engineering and Research, National Society of Earthquake Technology, Nepal*

⁴ *Doctoral student, Meguro laboratory, Institute of Industrial Science, the University of Tokyo, Japan*

⁵ *Director, International Center for Urban Safety Engineering, Institute of Industrial Science, the University of Tokyo, Japan*

Email: kawin@iis.u-tokyo.ac.jp

ABSTRACT :

In this study, we have proposed a new 3-D Applied Element Method (AEM) as an analysis tool for understanding the polypropylene band retrofitted masonry behavior which will be benefit in the future design process and increase the degree of freedoms of failure mode. Unlike the previous version of 3-D AEM, elements can be any rectangular prism which helps reducing the number of elements. Brick and mortar springs are represented by using different spring properties. Nonlinear constitutive law of the mortar spring employed the Gambarotta model which considers the material softening. Polypropylene band is modeled as beam element using plastic constitutive law connected together with the masonry by elastic spring representing the polypropylene band to brick connector. The numerical simulation of non-retrofitted and retrofitted out of plane wallets shows that with the suitable selected parameter the behavior of masonry can be closely reproduced.

KEYWORDS: Applied Element Method, Masonry, 3-D Simulation, Polypropylene band, Retrofit

1. INTRODUCTION

Masonry along with timber structures are among the oldest structures that are still used nowadays. Masonry structures history can be tracked back as early as 8,000-9,000 B.C. near Lake Hullen, Israel (Lourenço, 1996). With its long history, abundance of material, ease of construction and the advantages in thermal property, masonry is widespread used around the world. This type of structure still remains a main building material in many places especially in developing countries (Paola, 2003). Despite its advantages as residential structure, masonry is known as brittle and unsuitable for construction of buildings in seismic zones (Tomaževič, 1999). The 1997 Umbria-Marche, 1999 Bhuj and 2003 Bam earthquakes show that masonry is rather susceptible. A large number of masonry structures collapsed especially in concentrating area of poorly designed and constructed. Moreover, masonry structures collapse also result in high casualty because masonry tends to break into small debris and left insufficient void which reduce the chance of survival.

In order to improve the current situation, the proper retrofitting methods were invented. Several proposed retrofitting methods in the literatures include grout injection and internal reinforcing, ferrocement coatings, FRP composites and adding of steel elements. These methods were reported successfully for increasing the seismic capacity of the building. Besides them, the recent retrofitting scheme considering economic affordability and availability of material and skilled labor called Polypropylene band (referred hereafter as PP-band) retrofitting

technique has been proposed by Meguro's research group (Mayorca, 2003). Unlike the former methods, a main objective of this retrofitting technique is to hold the disintegrated elements together and preventing the collapse. In attempt to understand the behavior and to rationalize the design of these retrofitting methods, PP-retrofitted masonry wall testing was carried out. It was found that the behavior of the retrofitted walls was more stable and has larger deformation capacity compared to unretrofitted one. Moreover, the 2-D numerical model based on Applied Element Method (AEM) for simulating PP-band retrofitted wall was proposed using constitutive laws provided by Lorenço (1996). The group also conducted series of shaking table tests of the 1/4 scaled single unit masonry models with opening (Sathiparan, 2005). It was found that the retrofitted test models can resist up to 88 mm compared to 7 mm in an unretrofitted case for top displacement without collapse. Later, AEM was enhanced by adopting the constitutive laws from Gambarotta (1997) which make it able to simulating the in-plane cyclic behavior of PP-band retrofitted masonry (Guragain, 2006).

By considering the damage mechanisms in the masonry structures, the typical damage mechanism in the masonry structure can be identified as 1) cracks between walls and floors, 2) cracks at the corners and at wall intersections, 3) out-of-plane collapse of perimetral walls, 4) cracks in spandrel beams and/or parapets and 5) diagonal cracks in structural walls (Tomažević, 1999). Except the diagonal cracks, most masonry damage behavior inevitably relates with three dimensional behavior. With the proposed PP-band retrofitting, the interaction between each wall will be higher and therefore the seismic resisting mechanism tends to become more important. Moreover, because PP-band stiffness is much lower than masonry, the effect of retrofitted PP-band will play more significant role when a structure largely deforms. This is inevitably required the good understanding of three dimensional seismic behavior of masonry structure in the large deformation state. Despite a number of numerical models for structural analysis, few are suitable to simulate masonry in the large deformation range and AEM is one of them. In this study, we will propose a new 3-D AEM, based on previous 2-D AEM for masonry and 3-D AEM for concrete, to simulate three dimensional behaviors for PP-band retrofitted masonry structure.

2. 3-DIMENSIONAL APPLIED ELEMENT METHOD

In AEM (Meguro and Tagel-Din, 1997), the structure is divided into rigid elements, carrying only the system's mass and damping, connected with normal and shear springs representing the material properties (Figure 1). The stress and strain fields are calculated from the spring deformations. 3-D AEM rigid elements with 6 degrees of freedoms each element is connected through sets of one normal and two shear springs.

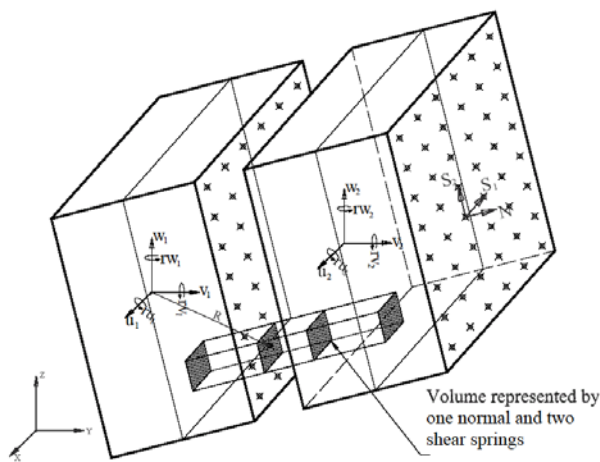


Figure 1 3 Dimensional AEM

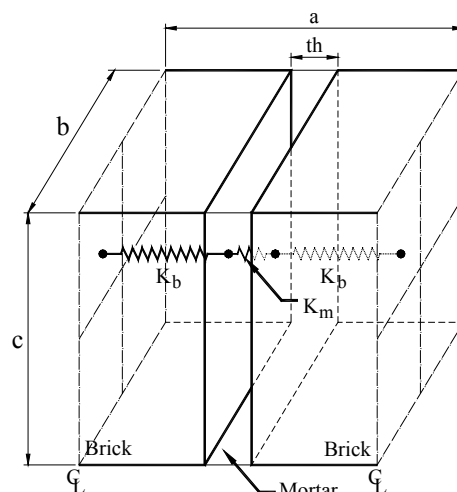


Figure 2 Concept of equivalent brick-mortar spring

3-D AEM used an explicit scheme to solve structural problems therefore it is required to assemble the system

stiffness matrix. For this purpose, it is necessary to sum up the contributions of all the springs around one element to the relevant degrees of freedom. Because each element has six degrees of freedom, the stiffness matrix of each spring is a 12 by 12 matrix which its components were generated by direct stiffness method.

Masonry is constituted by two phases: brick and mortar. Therefore, there are two types of springs: one inside brick units, brick spring, and the other at the joint interface, brick-mortar spring, are defined in 3D-AEM. In this paper, the brick spring stiffness is assumed to be elastic and its stiffness can be calculated as:

$$K_n = \frac{E \times b \times c}{a} \quad \text{and} \quad K_s = \frac{G \times b \times c}{a} \quad (1)$$

where E and G are Young's and shear modulus of brick, respectively. Other variables are shown in Figure 2. For the brick-mortar springs, an equivalent normal and shear stiffness is calculated by assuming that these springs represent a system of brick and mortar springs arranged in series as shown in Figure 2. The corresponding equivalent stiffness is:

$$\frac{1}{K_{n_{eq}}} = \frac{a-th}{E_b \times b \times c} + \frac{th}{E_m \times b \times c} \quad (2)$$

$$\frac{1}{K_{1s_{eq}}} = \frac{a-th}{G_b \times b \times c} + \frac{th}{G_m \times b \times c} \quad (3)$$

$$\frac{1}{K_{2s_{eq}}} = \frac{a-th}{G_b \times b \times c} + \frac{th}{G_m \times b \times c} \quad (4)$$

where E_b and G_b are the Young's and shear modulus of brick and E_m and G_m for the mortar. Eigenvalue analysis is also possible with the current version of 3-D AEM. The vector iteration with shifts technique is adopted. This technique is chosen as it provides a practical tool for computing as many pairs of natural vibration frequencies and modes of the structure as desired.

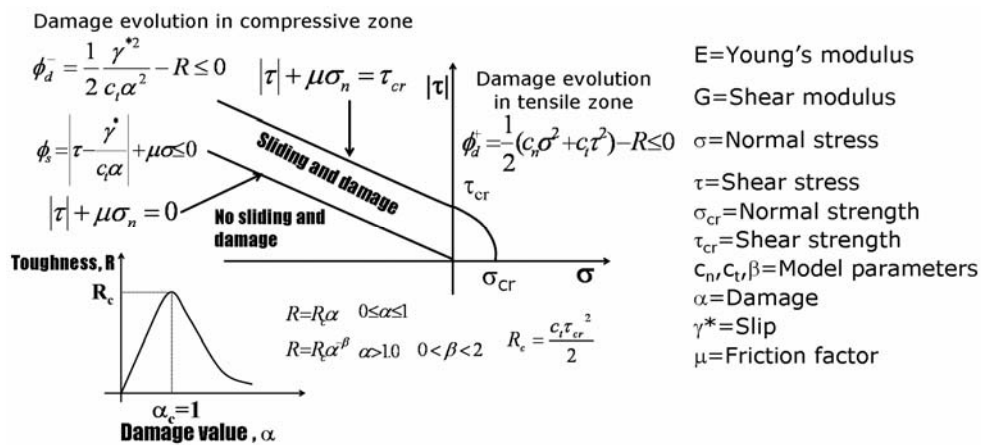


Figure 3 Constitutive relation to model the cyclic behavior of masonry

2.1 Masonry Modeling

The material constitutive relation requires spring level stress/strain updating for each loading step in the 3-D AEM. The stiffness changes in accordance to damage that material sustained in local level is required to monitor throughout the loading history. As mentioned earlier, the constitutive law needed to be modified in order to take into account this phenomenon. Such a model should be able to reflect the highly nonlinear

behavior of masonry with the fewest number of parameters so that it results in a simple and stable numerical model. Considering these criteria, the damage model of brick masonry proposed by Gambarotta et al (1996) has been chosen to implement in the 3D-AEM for cyclic behavior of the masonry. This constitutive law is able to reflect the important physical phenomena exhibited by masonry under cyclic loading.

The chosen constitutive model is based on damage mechanics and takes into account both the mortar damage and brick-mortar de-cohesion which is considered to take place when opening and frictional sliding are activated. Constitutive property of joint springs is based on two damage variables representing frictional sliding and mortar joint damage. Those variables are obtained from Mohr-Coulomb's friction surface and damage condition based on fracture mechanics. The damage evolutions in tensile and compression zones as well as the frictional limit criteria are given in Figure 3.

Stress at any springs can be defined as:

$$\{\sigma\} = [D] \{\varepsilon\} \quad (5)$$

Strain in springs can be split into elastic and plastic strain as:

$$\{\varepsilon\} = [K_e] \{\sigma\} + \{\varepsilon_p\} \quad (6)$$

where $[K_e]$ is the elastic compliance matrix of the spring. The plastic strain $\{\varepsilon_p\}$ can be written in as $\{\varepsilon_{np}, \gamma_p\}^t$ which is the result of inelastic normal and tangential displacement. Strain components are defined as functions of the damage variable α ,

$$\varepsilon_{np} = h(\alpha) H(\sigma_n) \sigma_n \quad (7)$$

$$\gamma_p = k(\alpha) (\tau - f) \quad (8)$$

where $h(\alpha)$ and $k(\alpha)$ are positive functions representing inelastic compliances in normal and tangential direction. $H(\sigma_n)$ is the heaviside function used to make the expression unilateral in tensile straining action and f is the friction developed at the interface between mortar and brick. Evaluation of the variable α and friction f is made through the limiting conditions of damage and friction sliding.

The damage condition based on R-curve approach of fracture mechanics is defined on the basis of energy release rate of damage, Y and toughness, R as:

$$\begin{aligned} \phi_d &= Y - R \leq 0 \\ Y &= (1/2) h'(\alpha) H(\sigma_n) \sigma_n^2 + (1/2) k'(\alpha) (\tau - f)^2 \end{aligned} \quad (9)$$

and the compliance functions $h(\alpha)$ and $k(\alpha)$ are assumed linear function of inelastic compliance constants as follows:

$$\begin{aligned} h(\alpha) &= c_n \alpha \\ k(\alpha) &= c_t \alpha \end{aligned} \quad (10)$$

The toughness function, R is related to damage evolution and is defined in terms of damage index α setting to attain its peak value R_c at critical value of $\alpha = \alpha_c (=1)$ and vanishing to zero as α increasing. The friction sliding condition is obtained from Mohr-Coulomb friction condition as:

$$\phi_s = |f| + \mu \sigma_n \leq 0 \quad (11)$$

where μ is friction coefficient and $|f|$ represents the shear component in surplus to cohesion.

2.2 PP-Band Mesh Modeling

The PP-band mesh is modeled through beam elements spanning between band intersections points as shown in Figure 4. These ends were then connected to the masonry structure through a set of three springs: normal, shear, and rotational. By appropriately setting the properties of these springs, it is possible to consider all possible connecting conditions between mesh and structure. For instance, if there is a wire connector at that particular location, all three springs have values proportional to the connector properties. On the other hand, if there is no connector and no mortar overlay, the normal spring only works in compression, i.e. when the mesh and the structure are in contact. As for the shear and rotation springs, their values are almost zero. This would not be the case if there was mortar overlay.

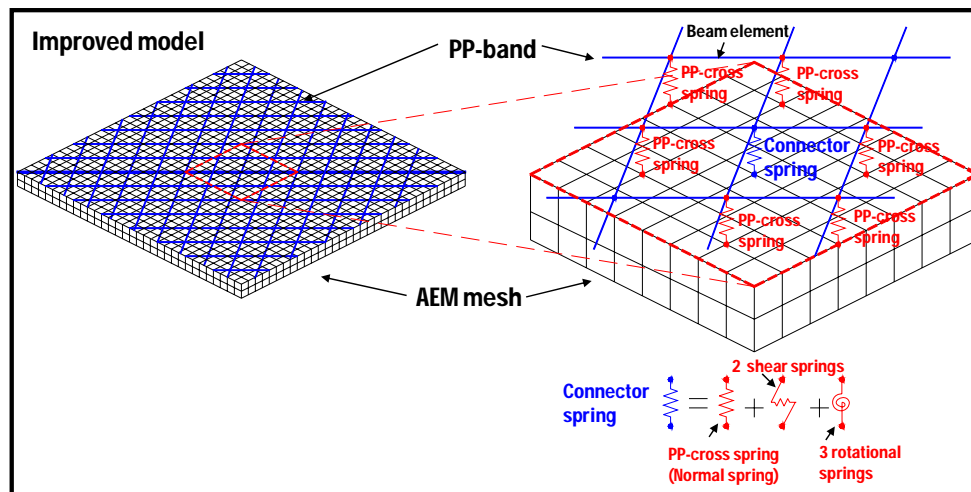


Figure 4 3D-AEM mesh modeling

The direct implication of a model as the one described above is the considerable increase of degrees of freedom of the system because each intersection point is associated with six more degrees of freedom. A 3-dimensional analysis by itself also involves the solution of systems with large number of degrees of freedom. Therefore, it is absolutely necessary to optimize the algorithms used to solve the equations of motion. This step is successfully implemented.

The material model used for each PP-band beam element is elastic in tension as shown in Figure 5. No compression forces are taken by the beam element. The beam elements are defined so as to have almost no moment resistance at their ends.

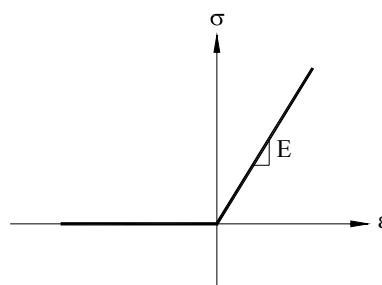


Figure 5 Material model for PP-band beam element

3. MODEL VERIFICATION

The 3D-AEM model is verified using the experimental data obtained by Sathiparan (2005). The non-retrofitted and retrofitted wallettes, shown in Figure 6 and Figure 7, are 475x235x50mm³ and consisted of 6 rows of 6 bricks each. The PP-band mesh is made of 6mm-width, 0.32mm-thick PP-bands placed at 40mm pitch. A total

of 6 wire connectors are used to attach the meshes to the wallettes. The wallettes are simply supported by high strength steel rods in both ends. The masonry wallettes are tested under line load using another steel rod of 200mm diameter in the mid span.

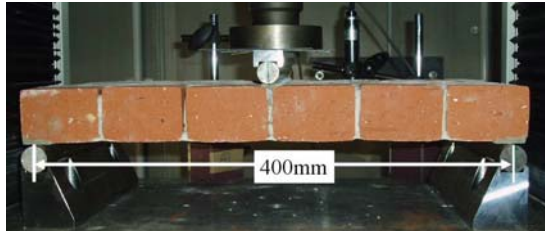


Figure 6 Retrofitted masonry wallette tested for out of plane

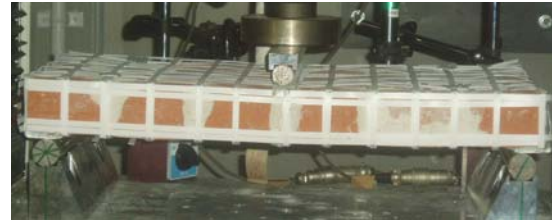


Figure 7 Boundary condition and loading of the masonry wallette for out of plane test

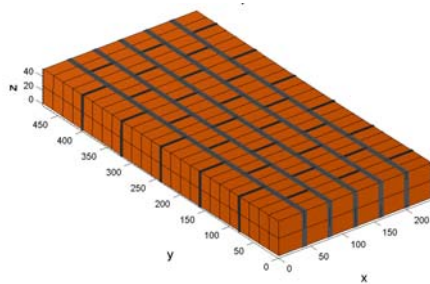
The material properties used for the masonry are summarized in Table 1. The PP-band mesh stiffness is set equal to 9.375 MPa.

Table 1 Material properties used for the modeling of out-of-plane masonry wallettes

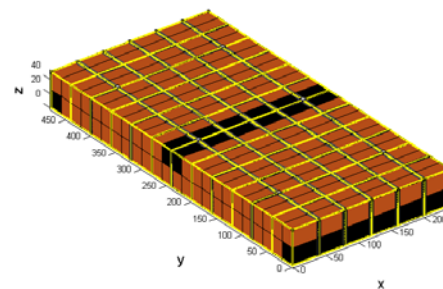
	Young's modulus E (kN/mm ²)	Shear modulus G (kN/mm ²)	Tensile strength σ_{cr} (kN/mm ²)	Shear strength τ_{cr} (kN/mm ²)	Friction coeff. μ	β	$1/C_{mt}$ (kN/mm ²)
Mortar	0.5	0.25	$0.16e^{-3}$	$0.22e^{-3}$	0.6	0.9	1/30
Brick	15.0	7.5	NA	NA	NA	NA	NA

NA: Not applicable

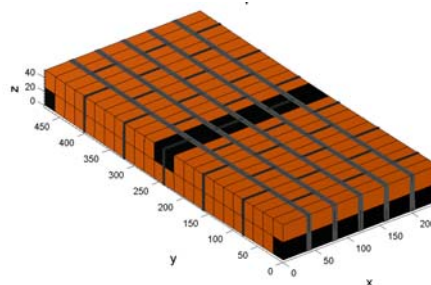
The models used for non-retrofitted and retrofitted models are shown in Figure 8.



(a) Non-retrofitted wallette



(b) Retrofitted wallette



(c) Boundary and loading condition
 (top dark elements: loading point, bottom dark elements: support)

Figure 8 Boundary condition and loading of the masonry wallette for out of plane test

Figures 9 and 10 show the comparison of numerical and experimental simulations for non-retrofitted and retrofitted wallets, respectively. It can be seen that in both cases, the model can accurately capture the force-deformation relationships.

The agreement between experiments and numerical simulation can also be observed in the crack patterns and deformed shapes (Figure 11).

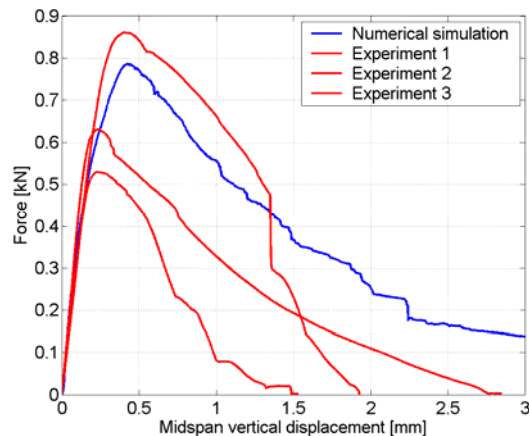


Figure 9 Numerical and experimental force-deformation curves for non-retrofitted wallets. (Experiments by Sathiparan, 2005)

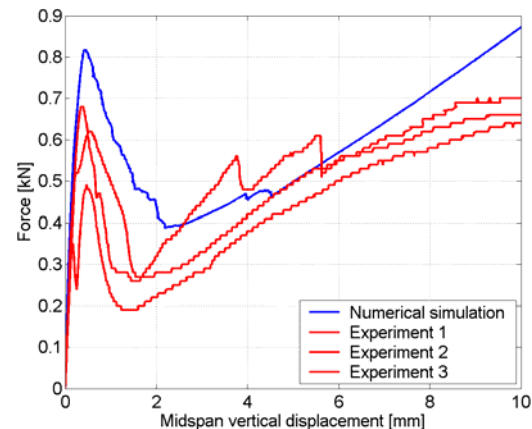


Figure 10 Numerical and experimental force-deformation curves for retrofitted wallets. (Experiments by Sathiparan, 2005)

4. CONCLUSION

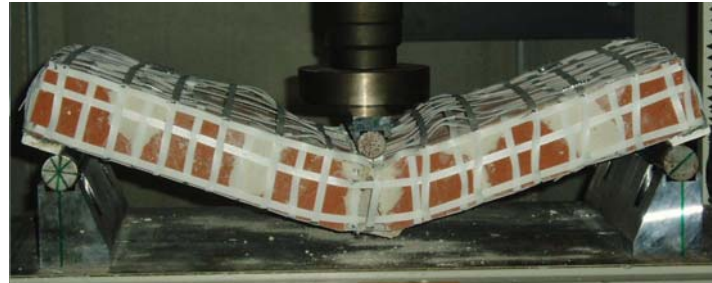
The 3-D AEM for simulating static behavior of PP-band retrofitted masonry was developed. The main improvements in this version are the rectangular prism AEM element which helps reducing the element number and the additional beam element and connected spring allowing AEM for simulating PP-band. The verification for 3-D AEM for PP-band retrofitted masonry for the out of plane test was carried out. The verification result showed that with the suitable selected parameter, the behavior of masonry could be closely reproduced.

REFERENCES

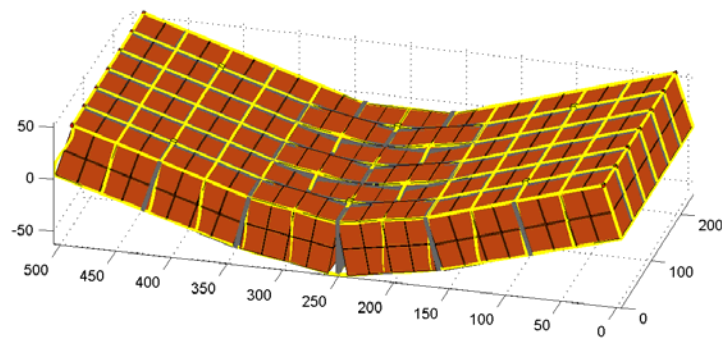
- Gambarotta L. and Lagomarsino S. (1997). Damage Response for the Seismic Response of Brick Masonry Shear Walls. Part I: The Mortar Joint Model and its Application. *Earthquake Engineering and Structural Dynamics*, **26**, 423-439
- Guragain, R. (2006), Numerical Simulation of Masonry Structures under Cyclic Loading using Applied Element Method, Master degree thesis, Department of civil engineering, The University of Tokyo.
- Lourenço, P.B. (1996), Computational Strategies for Masonry Structures, Delft University Press
- Mayorca, P. (2003), Strengthening of Unreinforced Masonry Structures in the Earthquake Pone Regions, Ph.D. thesis, Civil Eng. Dept., the University of Tokyo.
- Meguro, K., and Tagel-Din, H. (1997). Development and Application of New Model for Fracture Behavior Analysis of Structures. First US-Japan Workshop on Earthquake Engineering Frontiers in Transportation Facilities, Buffalo, New York, U.S.
- Tomažević, M. (1999). Earthquake-Resistant Design of Masonry Buildings, Imperial College Press, London,

U.K.

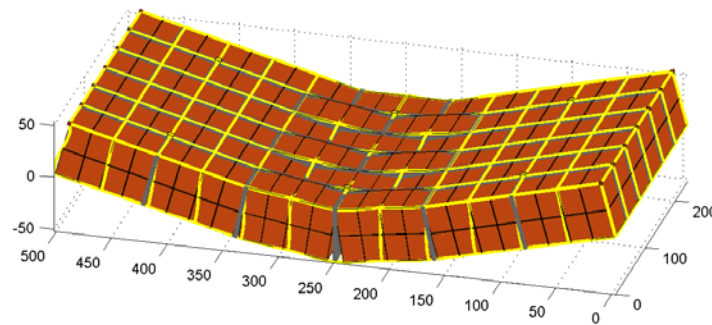
Sathiparan, N. (2005). Experimental study of retrofit of masonry building by pp-band mesh, Master degree thesis, Department of civil engineering, The University of Tokyo.



(a) Experiment



(b) Numerical simulation (scale factor: 20, midspan vertical displacement=3mm)



(c) Numerical simulation (scale factor: 5, midspan vertical displacement=10mm)

Figure 11 Comparison of numerical simulation and experimental results deformed shapes for retrofitted masonry